PERGAMON

International Journal of Heat and Mass Transfer 44 (2001) 4139–4146

International Journal of HEAT and MASS TRANSFER

www.elsevier.com/locate/ijhmt

Analysis of micro-Couette flow using the Burnett equations

H. Xue [a,*,1], H.M. Ji [b], C. Shu [b]

[a] *Mechanical Engineering Department, California State Polytechnic University, Pomona, 3801 West Temple Avenue, Pomona, CA 91768, USA*

[b] *Department of Mechanical and Production Engineering, National University of Singapore, 10 Kent Ridge Crescent, Singapore 119260, Singapore*

Received 24 November 1999; received in revised form 26 May 2000

Abstract

Analysis of micro-Couette flow and heat transfer is carried out using the Burnett equations. The generalized differential quadrature (GDQ) method is used to obtain the numerical solutions. The results show that the effect of the rarefaction is significant on velocity, temperature, pressure and non-dimensional parameter $Pr \cdot E$ for $Kn \geqslant 0.1$. The relationships between the shear stress, heat flux and Kn number are obtained. The solution of the Burnett equations is superior than that of the Navier–Stokes equations at the relatively high Kn number in the slip flow regime. However, it is impossible to extend the Burnett equations to the entire transition flow regime.

1. Introduction

Rarefied gas flows are encountered both in low pressure or vacuum environments and in micron or submicron size geometry at standard atmospheric conditions. The second category includes the application in micro-electro-mechanical-systems (MEMS). As the rarefaction increases, the continuum-based solution for the Boltzman equation may break down. The deviation of the state of the gas from continuum is measured by the Knudsen number, which is defined as $Kn = \lambda/L$, where λ is the mean free path of the molecules and L is a characteristic length scale. For $Kn \leqslant 10^{-3}$, the fluid can be considered as a continuum, the constitutive relations used in the continuum formulation are valid. For $Kn \geqslant 10$, it is considered as a free molecular flow, the Boltzman equation can be simplified into the classical Knudsen's model, which is valid for free molecular flow. In modeling the microscopic gas flow in MEMS, we mainly refer to those encountered from the slip flow regime ($10^{-3} < Kn < 0.1$) to the transition flow regime ($0.1 < Kn < 10$).

The Couette flow problem is one of the simplest problems in rarefied gas dynamics. However, no exact solution of the Boltzman equation has been found. The Chapman–Enskog method [1] provides a solution of the Boltzman equation for the Couette flow in which the distribution function f is perturbed by a small amount from the equilibrium Maxwellian form. The zeroth-order solution is the Maxwellian distribution function f_0 with the gas being fully described by density ρ, macroscopic velocity vector u, and temperature T. The viscous stress tensor σ_{ij} and the heat flux vector q_i vanish in an equilibrium gas and the conservation equations reduce to the Euler equations of inviscid fluid flow. The first-order Chapman–Enskog solution leads to the velocity distribution function, which enables σ_{ij} and q_i to be written as products of the coefficients μ and k with the velocity and temperature gradients. Thus the conservation equations reduce to the Navier–Stokes equations. The second-order Chapman–Enskog solution leads to the Burnett equations.

Since the zeroth-order and first-order Chapman–Enskog solutions merely reconcile the molecular and continuum approaches for small Knudsen flows, it is not difficult to understand that the deviation from the state

* Corresponding author. Tel.: +1-909-869-4304; fax: +1-909-869-4341.

E-mail address: hxue@csupomona.edu (H. Xue).

[1] Fax: +65-779-1459.

0017-9310/01/$ - see front matter
PII: S0017-9310(01)00062-X

Nomenclature

C	speed of sound ($=\sqrt{\gamma RT}$)
c_p	specific heat, J/kg K
E	Eckert number ($=u_1^2/(c_p(T_1-T_2))$)
H	distance between two parallel plates, m
K	thermal conductivity, W/m K
Kn	Knudsen number
L	characteristic length scale, m
M	Mach number ($=u_1/\sqrt{\gamma RT_1}$)
Pr	Prandtl number ($=c_p\mu/k$)
P	pressure, Pa
q_i	heat flux vector, W/m^2
R	gas constant, J/kg K
T	temperature, K
U	velocity component in the x-direction, m/s

Greek symbols

γ	specific heat ratio
λ	mean free path, m
μ	dynamic viscosity, kg/m s
ρ	density, kg/m^3
σ_{ij}	viscous stress tensor
σ_u, σ_T	accommodation coefficients
ω	exponent in viscous-temperature law

Superscripts and subscripts

s	surface next to the wall
w	wall
0	reference state
1	plate 1
2	plate 2
$\sim$	non-dimensional variable

of gas from continuum gets larger as Knudsen number increases from the slip flow regime to transition flow regime. Beskok and Karniadakis [2] suggested that the continuum approximations that include high-order modifications of the stress tensor and heat flux term, may be considered to substitute the Navier–Stokes equations in the transition flow regime. There is evidence [3] that use of the Burnett equations extends the validity of the continuum model to flows that are more rarefied than those for which the Navier–Stokes equations are valid. Moreover, studies showed that the Burnett equations can significantly improve the Navier–Stokes solutions for one-dimensional shock-structure problem and two-dimensional hypersonic blunt body flows [4–6].

The present study, therefore, intends to obtain numerical solutions of the Burnett equations for micro-Couette flow. An accurate numerical scheme, the generalized differential quadrature (GDQ) [7,8] is adopted to solve the Burnett equations. Investigation is focused on the flow and heat transfer behavior of the Couette flow. Comparisons are made with the solutions of the Navier–Stokes equations and other available data. The advantage of using Burnett equations and the limitation in the transition flow regime are discussed.

2. Steady Couette flow

We consider the flow between two parallel infinite flat plates (Couette flow), as shown in Fig. 1. The space between two infinite parallel plates is separated by a distance H. The lower plate (plate 1) at $y=0$ moves with a constant velocity u_1 and sets the fluid particles moving in the direction parallel to the plates while the upper plate (plate 2) remains stationary. The flow is considered steady, one-dimensional and compressible. The governing equations of the Navier–Stokes and the Burnett equations for the Couette flow are written as follows:

$$\frac{\mathrm{d}}{\mathrm{d}y}\begin{bmatrix}\sigma_{12}\\ p+\sigma_{22}\\ u\sigma_{12}+q_2\end{bmatrix}=0, \tag{1}$$

where u is velocity in x direction, and p is pressure. σ_{ij} and q_i are the deviatorial pressure tensor and heat flux, respectively.

For the Navier–Stokes equations, the expression of σ_{ij} and q_i are given, $\sigma_{12}=-\mu u'$, $\sigma_{22}=0$, $q_2=-kT'$, where μ is viscosity coefficient, k is thermal conductivity of the gas, and T is temperature. The superscript $'$ represents the first derivative with respect to y.

For the Burnett equations, σ_{12} and q_2 for the steady Couette flow are the same as those of the Navier–Stokes equations, but

$$\sigma_{22}=\frac{\mu^2}{p}\left(\alpha_6 u'^2+\alpha_7 RT''+\alpha_9\frac{RT}{\rho}\rho''+\alpha_{11}\frac{RT}{\rho^2}\rho'^2+\alpha_{12}\frac{R}{\rho}T''+\alpha_{13}\frac{R}{T}T'^2\right), \tag{2}$$

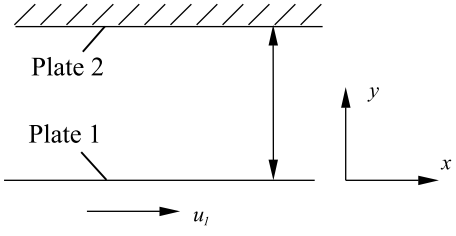

Fig. 1. Couette flow coordinate system.

where ρ is the density. The coefficients for Maxwellian gas are $\alpha_6 = -0.667$, $\alpha_7 = 0.667$, $\alpha_9 = -1.333$, $\alpha_{11} = 1.333$, $\alpha_{12} = -1.333$, $\alpha_{13} = 2.0$. The superscripts $''$ represents the second derivative with respect to y. For an ideal gas, the equation of state is given by

$$p = \rho RT. \tag{3}$$

From above equations, we can see that the Burnett equations have high-order modification of stress tensor and heat flux terms.

The variables in the equations governing the Couette flow are non-dimensionalized as follows. The reference variables are chosen according to [9]

$$\tilde{y} = \frac{y}{H}, \quad \tilde{u} = \frac{u}{\sqrt{RT_0}}, \quad \tilde{T} = \frac{T}{T_0}, \quad \tilde{\rho} = \frac{\rho}{\rho_0},$$
$$\tilde{p} = \frac{p}{p_0}, \quad \tilde{\sigma}_{ij} = \frac{\sigma_{ij}}{\rho_0 RT_0}, \quad \tilde{q}_i = \frac{q_i}{\rho_0 (RT_0)^{3/2}}, \quad \tilde{\mu} = \frac{\mu}{\mu_0},$$

where the subscript 0 denotes in the reference state.

After the non-dimensionlization, the Navier–Stokes equations become

$$\frac{\mathrm{d}}{\mathrm{d}\tilde{y}}(\tilde{\mu}\tilde{u}') = 0, \tag{4}$$

$$\frac{\mathrm{d}\tilde{p}}{\mathrm{d}\tilde{y}} = 0, \tag{5}$$

$$\frac{\mathrm{d}}{\mathrm{d}\tilde{y}}\left[(-\tilde{u}\tilde{\mu}\tilde{u}') + \frac{\gamma}{Pr(\gamma-1)}\tilde{\mu}\tilde{T}'\right] = 0, \tag{6}$$

where the Pr is the Prandtl number and γ is the specific heat ratio. For the Burnett equations, the y-momentum equation is different from Eq. (5), and is written as

$$\tilde{p} + Kn_0^2 \frac{\tilde{\mu}^2}{\tilde{p}}\left[\alpha_6\tilde{u}'^2 + \alpha_9\frac{\tilde{T}}{\tilde{p}}\tilde{p}'' + \alpha_{11}\frac{\tilde{T}}{\tilde{p}^2}\tilde{p}'^2 + (\alpha_{12} - 2\alpha_9 - 2\alpha_{11}) \times \frac{1}{\tilde{p}}\tilde{T}'\tilde{p}' + (\alpha_{13} + 2\alpha_9 + \alpha_{11} - \alpha_{12})\frac{1}{\tilde{T}}\tilde{T}'^2 + (\alpha_7 - \alpha_9)\tilde{T}''\right] = P_0, \tag{7}$$

where P_0 is an integration constant and Kn_0 is the reduced Knudsen number, which is defined with reference variables as

$$Kn_0 = \frac{\mu_0}{\rho_0\sqrt{RT_0}H}. \tag{8}$$

Two types of boundary conditions, namely non-slip wall and slip wall conditions are imposed in the calculation. For the non-slip wall, the fluid next to the wall moves with the plate, and the temperature takes on the prescribed wall temperature.

For the slip wall, the following first-order boundary conditions in non-dimensional form (Maxwell/Smolu-chowski slip conditions) are used. The effects of thermal creep and quadratical variation with Kn are not included.

$$\tilde{u}_s - \tilde{u}_w = \frac{2-\sigma_u}{\sigma_u}\sqrt{\frac{\pi}{2}}Kn_0\frac{\sqrt{\tilde{T}}\tilde{\mu}}{\tilde{p}}\left(\frac{\mathrm{d}\tilde{u}}{\mathrm{d}\tilde{y}}\right)_s, \tag{9}$$

$$\tilde{T}_s - \tilde{T}_w = \frac{2-\sigma_T}{\sigma_T}\frac{2\gamma}{Pr(\gamma+1)}\sqrt{\frac{\pi}{2}}Kn_0\frac{\sqrt{\tilde{T}}\tilde{\mu}}{\tilde{p}}\left(\frac{\mathrm{d}\tilde{T}}{\mathrm{d}\tilde{y}}\right)_s. \tag{10}$$

To carry out the numerical simulation, we assume that (1) the accommodation coefficients for $\tilde{u}$ and $\tilde{T}$ are $\sigma_u = 1$ and $\sigma_T = 1$, respectively; (2) the gas is the Maxwell molecular, for which the exponent ω in the viscosity-temperature law ($\tilde{\mu} = \tilde{T}^{\omega}$) is 1, Prandtl number ($Pr$) is 2/3, and the ratio of specific heat γ is 5/3; (3) the integral constant in Eq. (8) is $P_0 = 1$.

The numerical solutions of the Burnett equations in the continuum transitions regime have not been possible for flow with very fine grids since the Burnett equations are unstable to the disturbances of small wavelength [10]. An accurate numerical method with a possible coarse grid system is desired. Therefore, we selected the GDQ method [7,8] to solve the Burnett equations. The GDQ method discretizes spatial derivatives by a weighted linear sum of all the functional values in the whole domain. The GDQ method can be considered as the highest order finite difference scheme for a domain with a given mesh. Application of both GDQ and Chebyshev pseudo-spectral methods provides the same weighting coefficients for the first derivative when the grid points are chosen as the roots of the Nth order Chebyshev polynomial for the both methods.

Eqs. (4)–(7) are numerically solved by the GDQ method. Thirteen grid points are used along the y-direction. A grid refinement study has been carried out. The results show that 13 meshes yield an accurate independent solution. The convergence criterion for the simulation is based on the residual value for the continuity equation. The criterion ensures that the maximum residual $\left|\mathrm{Res}_{ij}^{n+1}\right|_{\max} \leqslant 10^{-4}$.

3. Results and discussions

3.1. Flow analysis

To examine the flow behavior, the velocity of moving plate is set at $\tilde{u}_1 = 1$, the temperatures at stationary and moving plate are $\tilde{T}_1 = \tilde{T}_2 = 1$, and the pressures are $\tilde{p}_1 = \tilde{p}_2 = 1$. The velocity, temperature and pressure distributions along the y-direction of the parallel plates are obtained.

Fig. 2 shows the solutions of velocity, temperature and pressure for the non-slip boundary condition. It is

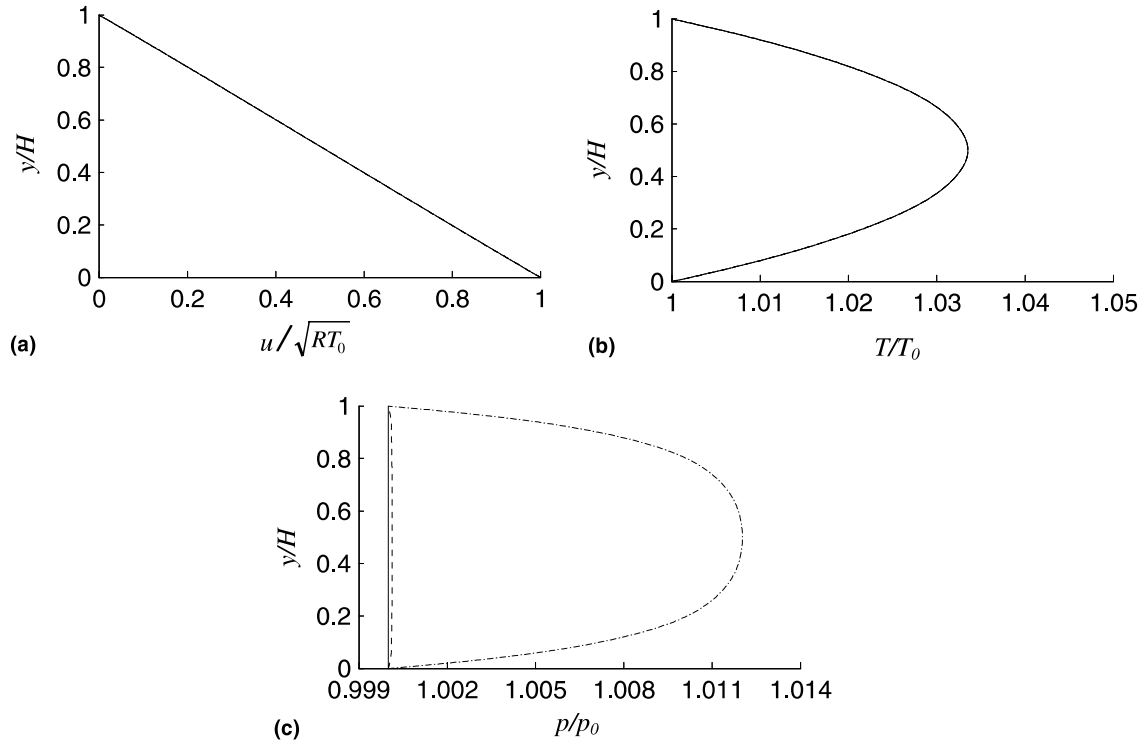

Fig. 2. Numerical solution for non-slip wall conditions: (a) velocity $\tilde{u}$; (b) temperature $\tilde{T}$; (c) pressure $\tilde{p}$.

noted that when the non-slip condition is imposed, the Navier–Stokes equations and the Burnett equations at $Kn = 0$, $Kn = 0.01$ and $Kn = 0.1$ yield the same solutions for $\tilde{u}$ and $\tilde{T}$, due to the decoupled relations between $\tilde{u}$, $\tilde{T}$ and $\tilde{p}$. But the pressure is different. For the Navier–Stokes equations, the pressure is a constant, the fluid motion is set by simple shear flow due to viscosity, and no pressure gradient is involved in the direction of motion. It is also a constant along the y-direction. But the Burnett equations yield the pressure gradient in the y-direction due to the high-order modification. There are wall layers near both upper and lower plates with the thickness estimated to be of the order of Kn, because the highest derivative term is multiplied by Kn^2. As indicated in Fig. 3, the wall layer is a very thin layer (about one to a few mean free paths) next to the wall, and is also known as the Knudsen layer. The wall layers will not vanish as long as Kn number is not zero.

The solutions of velocity, temperature and pressure for the Burnett equations with the first-order slip boundary conditions are given in Fig. 4. In Fig. 4(a), the velocity at the lower wall is lagged behind the moving plate, while the velocity at the upper wall is stretched due to the slip effect. But the velocity profile is still kept in linear. The temperature in slip flow is higher than that in non-slip flow as indicated in Fig. 4(b). The pressure profile Fig. 4(c) has the same trend as that in non-slip condition. Overall, when $Kn = 0.01$, the difference in the velocity, temperature and pressure distributions with those at $Kn = 0$ is very limited. As the Knudsen number increases to 0.1, the difference becomes larger.

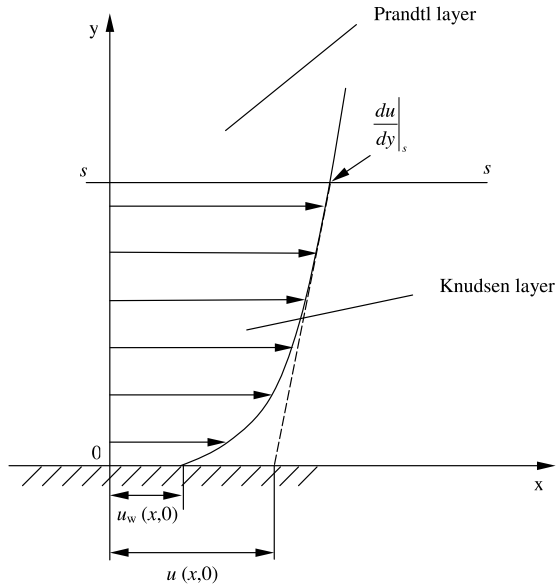

Fig. 3. Near-wall velocity distribution.

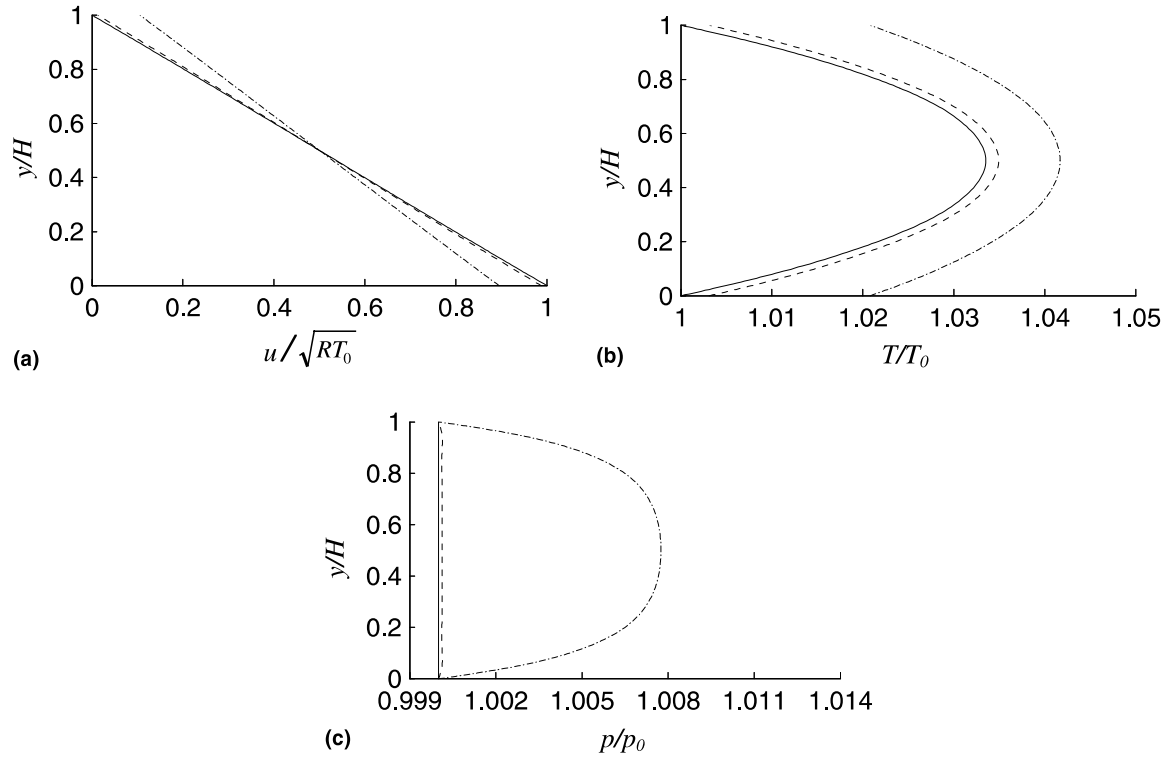

Fig. 4. Numerical solutions for slip wall conditions: (a) velocity $\tilde{u}$; (b) temperature $\tilde{T}$; (c) pressure $\tilde{p}$.

To examine the performance of the Burnett equations, Fig. 5 shows relationship between the non-dimensional shear stress and the Knudsen number at $M = 3$, at which the solution of the six-moment method by Liu and Lees [11] and the solution of direct simulation by Nanbu [12] were available for comparison. $M\ (= u_1/\sqrt{\gamma RT_1})$ is the wall Mach number. In Figs. 5 and 9 shown later, the results of the Navier–Stokes equations and the Burnett equations are all obtained with velocity slip and temperature jump conditions at different Kn numbers. It is clear that the Navier–Stokes equations are only accurate in the region where $Kn < 0.04$. Similar to the solution of the six-moment method, the result of the Burnett equations is close to the solution of the direct simulation in the region up to about $Kn = 0.1$. However, we were not able to obtain solutions for the Burnett equations with the first-order slip boundary conditions after Knudsen number reaches 0.18. Failed in many attempts to try possible relaxation on the numerical scheme, we believed that the failure is not due to the numerical flaw but the physical one. The inability of the continuum approaches with slip boundary conditions in predicting flow in the transition flow regime is attributed to the physical changes in the Knudsen layer. From Fig. 3, it is not difficult to imagine that the error of using the slip velocity to approximate the real velocity at the wall $u_w\ (x, 0)$ would significantly increase as the Knudsen layer becomes comparable thick to the distance between plates 1 and 2. As indicated in Fig. 5, the gradient of the shear stress becomes nonlinear after the Knudsen number reaches 0.04, and the shear stress approaches asymptotically to the free molecular limit as $Kn \to \infty$. Hence, the assumption on the Knudsen number as a linear coefficient of the slip velocity and temperature jump in Eqs. (9) and (10) is only valid for the Knudsen number less than 0.04.

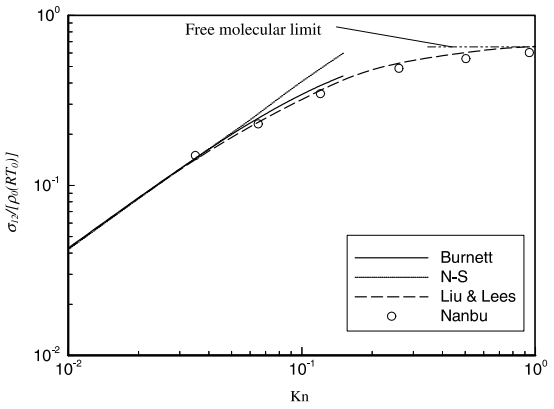

Fig. 5. Shear stress as a function of Kn for $M = 3$.

Although the Burnett equations can improve the prediction of the Navier–Stokes equations in the region from $Kn = 0.04$ to about $Kn = 0.1$, it is impossible to further extend the Burnett equations to the entire transition flow region. In fact, even if the second-order slip boundary condition developed by Schamberg [13] are used, the numerical simulation with aerodynamic rarefied flow [6] showed that Scamberg's boundary conditions were inaccurate for $Kn > 0.2$.

3.2. Heat transfer

Heat transfer is an important issue in the Couette flow. Since viscous energy dissipation may become considerable even at moderate flow velocities, the temperature rise in the fluid and the amount of heat transfer through the plates are of interest. To examine the effect of the rarefaction on heating of the walls, three different temperature ratios of lower plate to upper plate are prescribed at 1, 2, and 20, respectively. Fig. 6 shows the temperature variations with the distance between the upper and lower plates. The slip velocity and temperature jump conditions are imposed to the Burnett equations, except for the case $Kn = 0$. From Figs. 6(a) and (b), it is observed that when the temperature ratio is small, the deviation of the case $Kn = 0$ from the cases $Kn = 0.01$ and $Kn = 0.1$ is relatively small. The effect of rarefaction on the heating is insignificant. At large temperature ratio, however, the temperature jump becomes distinguish at higher Knudsen numbers as shown in Fig. 6(c).

In classical heat transfer, the direction of heat flow at the lower plate, that is, whether the heat flow is into the fluid or the wall for $T_1 > T_2$, depends on the magnitude of the non-dimensional parameter $Pr \cdot E$ [14], where Pr is the Prandtl number and E is the Eckert number. The relationship between the non-dimensional temperature and parameter $Pr \cdot E$ is shown in Fig. 7. For $Pr \cdot E > 2$, the heat flows in the negative y-direction, even through the lower plate is at a higher temperature than that of the upper plate. For $Pr \cdot E < 2$, the heat flows in the positive direction. For $Pr \cdot E = 2$, there is no heat flow at the lower wall. From Fig. 8, it is interesting to see that the non-dimensional parameter $Pr \cdot E$ is deviated from the value 2, at which the heat flow is set to be zero at the lower wall, as the rarefaction increases. Subsequently, the value for $Pr \cdot E$ becomes 2.008 at $Kn = 0.01$, 2.011 at $Kn = 0.05$ and 2.1505 at $Kn = 0.1$. This implies that to keep the lower wall not heated, the moving velocity of the plate must increase as the gaseous flow becomes more rarefied. Compared with the results of the Navier–Stokes equations, there are temperature jumps at the lower and upper walls in Fig. 8. With the increase of the Knudsen number,

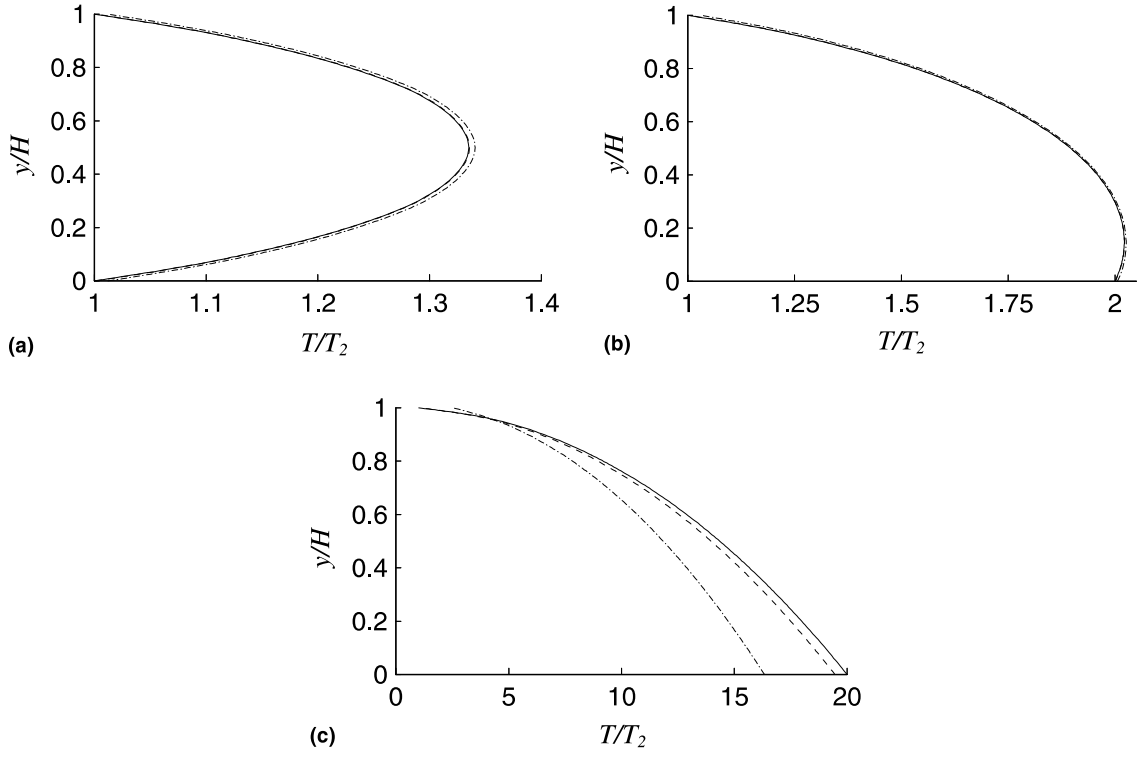

Fig. 6. Effect of rarefaction on heating at different temperature ratios: (a) $T_1/T_2 = 1$; (b) $T_1/T_2 = 2$; (c) $T_1/T_2 = 20$.

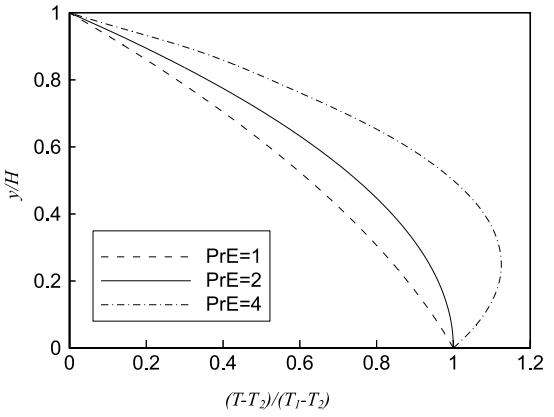

Fig. 7. Non-dimensional temperature distribution (Navier–Stokes equations with non-slip wall conditions, $Kn = 0$).

the temperature jump becomes pronounced. Taking the curve of $Pr \cdot E = 1$ as an example, the temperature jump at the lower wall is 0.004 at $Kn = 0.001$, 0.017 at $Kn = 0.05$ and 0.028 at $Kn = 0.1$. When the non-dimensional parameter $Pr \cdot E$ increases from 1 to 4, the temperature jump experiences the change from negative to positive. For example, in Fig. 7(c), the temperature is unity at $Pr \cdot E = 2.1505$, if $Pr \cdot E < 2.1505$, the temperature jump is negative, while for $Pr \cdot E > 2.1505$, the temperature jump becomes positive.

Corresponding to Fig. 5, the non-dimensional heat flux is plotted in Fig. 9 together with the solutions of six-moment method [11] and the direct simulation [12]. The prediction of the Navier–Stokes equations is only good in the region where $Kn < 0.02$. The Burnett equations extend the region to about $Kn = 0.1$, but fail to predict the heat flux as the Knudsen number increases to 0.18. The direct simulation result [12] shows that heat flux reaches the peak at $Kn = 0.2$, and it decreases asymptotically to zero as $Kn \to \infty$. This indicates that the assumption on the Knudsen number as the coefficient of the slip velocity and temperature jump is only valid when the Knudsen number is sufficient small. As

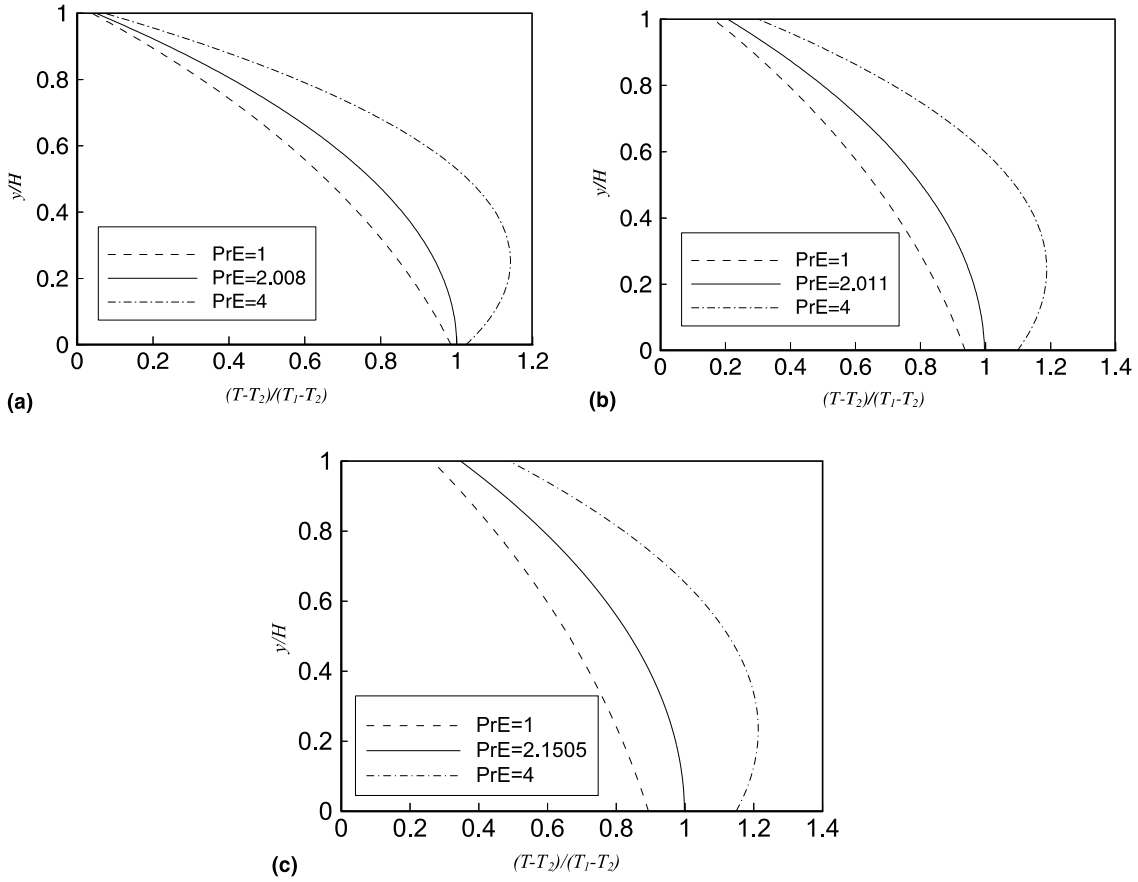

Fig. 8. Non-dimensional temperature distribution (Burnett equations with slip wall conditions): (a) $Kn = 0.01$; (b) $Kn = 0.05$; (c) $Kn = 0.1$.

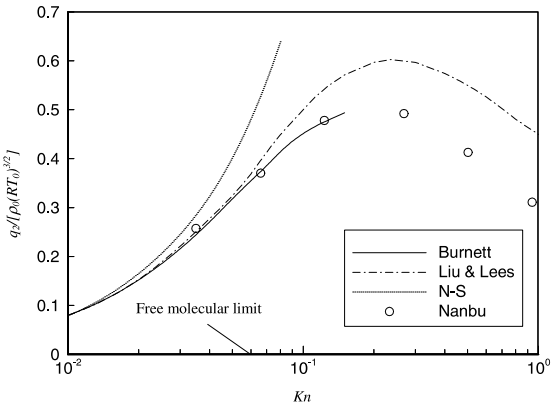

Fig. 9. Heat flux as a function of Kn for $M = 3$.

explained previously, the failure of the Burnett equations is due to the limitation of the proportional relationship between temperature jump and the Knudsen number.

4. Conclusions

Numerical solutions of the Burnett equations for Couette flow have been obtained using the GDQ method. The GDQ method provides us a simple but accurate numerical solution to deal with the microscopic Couette flow using the Burnett equations where the higher order of the Chapman–Enskog expansion is required.

The Characteristics of the gaseous Couette flow and heat transfer are analyzed. The study shows that there is significant effect of rarefaction on the distribution of velocity, temperature and pressure when the flow enters the transition regime for isothermal wall or when the temperature ratio is high for non-isothermal wall. The value of non-dimensional parameter $Pr \cdot E$, at which heat flow becomes zero at the heated wall, is no longer a constant in micro-Couette flow. It increases as the Knudsen number becomes larger.

The solution of the Burnett equation is superior than that of the Navier–Stokes equations at relatively high Knudsen number in the slip flow regime. However, it is impossible for the Burnett equation to be extended to the entire transition flow regime, as long as the assumption on the Knudsen number as the coefficient of the slip velocity and temperature jump is made.

Acknowledgements

This research is supported by the academic research fund, RP3981677, National University of Singapore.

References

[1] S. Chapman, T.G. Cowling, The Mathematical Theory of Non-Uniform Gases, third ed., Cambridge University Press, England, UK, 1970.
[2] A. Beskok, G.E. Karniadakis, A model for flows in channels, pipes, and ducts at micro and nano scales, Microscale Thermophys. Eng. 3 (1999) 43–77.
[3] K.A. Fiscko, D.R. Chapman, Comparison of Burnett, super-Burnett and Monte Carlo solutions for hypersonic shock structure, Prog. Aero. Astro. 118 (1989) 374–495.
[4] G.C. Pham-Van-Diep, D.A. Erwin, E.P. Muntz, Testing continuum descriptions of low Mach number shock structures, J. Fluid Mech. 232 (1991) 403–413.
[5] F.E. Lumpkin III, Accuracy of the Burnett equations for hypersonic real gas flows, J. Thermophys. Heat Transfer 6 (3) (1992) 419–425.
[6] X.L. Zhong, On numerical solutions of Burnett equations for hypersonic flow past 2-D circular blunt leading edges in continuum transition regime, in: AIAA 42 Fluid Dynamic Conference, AIAA 93-3092, Orlando, 1993.
[7] C. Shu, B.C. Khoo, K.S. Yeo, Numerical solutions of incompressible Navier–Stokes equations by generalized differential quadrature, Finite Elements Anal. Design 18 (1994) 83–97.
[8] C. Shu, Generalized differential-integral quadrature and application to the simulation of incompressible viscous flows including parallel computation, Ph.D. thesis, University of Glasgow, UK, 1991.
[9] C.J. Lee, Unique determination of solutions to the Burnett equations, AIAA J. 32 (5) (1994) 985–990.
[10] X.L. Zhong, R.W. MacCormack, D.R. Chapman, Stabilization of the Burnett equations and application to hypersonic flows, AIAA J. 31 (6) (1993) 1036–1043.
[11] C.Y. Liu, L. Lees, Kinetic theory description of plane compressible Couette flow, in: L. Talbot (Ed.), in: Rarefied Gas Dynamics, Academic Press, New York, 1961, pp. 391–428.
[12] K. Nanbu, Analysis of the Couette flow by means of the new direct-simulation method, J. Phys. Soc. Jpn. 52 (5) (1983) 1602–1608.
[13] R. Schamberg, The fundamental differential equations and the boundary conditions for high speed slip-flow, and their application to several specific problems, Ph.D. thesis, California Institute of Technology, USA, 1947.
[14] M.N. Ozisik, Heat Transfer, McGraw-Hill, New York, 1985.